Least-squares reverse-time migration using one-step two-way wave extrapolation by non-stationary phase shift

Junzhe Sun, Sergey Fomel, and Jingwei Hu, The University of Texas at Austin*

Downloaded 11/06/14 to 128.210.3.233. Redistribution subject to SEG license or copyright; see Terms of Use at http://library.seg.org/

SUMMARY

The one-step low-rank wave-extrapolation operator is a non-stationary combination filter, and, as such, corresponds to the well-known PSPI method for the one-way wave equation. We propose its adjoint operator, the non-stationary phase shift (NSPS) wave extrapolation in time, which is a non-stationary convolution filter. A combination of PSPI and NSPS methods creates a symmetric and more accurate wave propagator. Numerical examples using a two-layer model demonstrate the improved accuracy. For applications to prestack reverse-time migration (RTM), the proposed framework incorporates a complex valued imaging condition. We use the forward modeling operator and its adjoint to implement least-squares RTM (LSRTM). Synthetic examples illustrate that, compared with conventional RTM, the low-rank LSRTM is capable of suppressing migration artifacts and achieving better illumination.

INTRODUCTION

Wavefield extrapolation in time is the kernel of reverse-time migration (RTM), which is capable of accurately imaging geologically complex media by directly solving the two-way wave equation (Baysal et al., 1983; McMechan, 1983; Whitmore, 1983; Farmer et al., 2006; Fletcher et al., 2009; Fowler et al., 2010a). Because of its high efficiency, finite-difference method is the most popular approach for wave propagation, however that method suffers from instabilities and dispersion artifacts (Kosloff and Baysal, 1982). Pseudo-spectral methods calculate space derivatives by using Fourier transforms and are more accurate, but those methods still suffer from grid dispersion due to finite-difference approximation on the time axis (Reshef et al., 1988). Recently, a lot of research has been done to develop the mixed-domain space-wavenumber operators (Zhang et al., 2007; Soubaras and Zhang, 2008; Etgen and Brandsberg-Dahl, 2009; Liu et al., 2009; Stoffa and Pestana, 2009; Zhang and Zhang, 2009; Chu and Stoffa, 2010; Du et al., 2010; Fowler et al., 2010b; Pestana and Stoffa, 2010; Fomel et al., 2013; Song et al., 2013), which are described by Du et al. (2014) as recursive integral time extrapolation (RITE) because they are based on formal integral solutions of the wave equation. RITE methods are capable of propagating wavefields free of instability and dispersion even at large time steps, and thus are suitable for RTM. The imaging problem can also be viewed as an inverse problem (Ronen and Liner, 2000). Least-squares migration using Kirchhoff migration, one-way wave-equation migration and RTM engines, can be used to improve the quality of image produced by conventional methods (Nemeth et al., 1999; Tang, 2009; Dai et al., 2011; Zhang et al., 2013; Liu et al., 2013).

Among different RITE methods, the low-rank method proposed by Fomel et al. (2013) stands out for its high accuracy and flexible control over the trade-off between efficiency and approximation accuracy. A low-rank algorithm approximates the original space-wavenumber propagation matrix with the product of low-rank matrices using a small set of representative rows and columns, with the computational cost of $O(N N_x \log N_x)$, where N_x is the total size of the three-dimensional grid and N is the rank of the approximation, which is usually a small number. Sun and Fomel (2013) extended the low-rank method to one-step wave propagation (Zhang and Zhang, 2009), and demonstrated advantages of a one-step scheme over a two-step scheme in terms of numerical stability and wave propagation accuracy.

The one-step low-rank wave extrapolation for the two-way wave equation resembles the well-known phase shift plus interpolation (PSPI) method for the one-way wave equation (Gazdag and Squazzero, 1984; Kesinger, 1992). From the perspective of non-stationary linear filtering (Margrave, 1998), in the limit of an exhaustive set of reference velocities, the PSPI method corresponds to a kind of non-stationary combination filter. For one-way wave equation, Margrave and Ferguson (1999) introduced the non-stationary phase shift (NSPS) wave extrapolation, which is the adjoint of PSPI and a form of non-stationary convolution filter. Following an analogous strategy, we propose a NSPS-like operator for the two-way wave extrapolation, as a non-stationary convolution filter. We also name it NSPS in the context of two-way wave extrapolation. We present the derivation of the NSPS operator using non-stationary filtering theory and employ low-rank decomposition to approximate it. We further propose to combine the low-rank one-step NSPS and PSPI operators to construct a symmetric operator with increased accuracy. Using a simple two-layer model (Du et al., 2014), we demonstrate the improved accuracy using the hybrid operator at large time steps. We supply the PSPI and NSPS operators for one-step low-rank wave extrapolation during RTM and least-squares RTM (LSRTM). LSRTM is applied on the Sigsbee2A model (Paffenholz et al., 2002) to illustrate the ability of LSRTM to remove image artifacts and improve illumination of deep reflectors.

THEORY

Let $p(\mathbf{x},t)$ be the seismic wavefield at location $\mathbf{x}$ and time t, with the spatial Fourier transform denoted by $P(\mathbf{k},t)$. The wavefield at the next time step $t+\Delta t$ can be approximated by the Fourier integral operator (Wards et al., 2008; Fomel et al., 2013):

$$p(\mathbf{x},t+\Delta t) = \int P(\mathbf{k},t)\, e^{i\,\phi(\mathbf{x},\mathbf{k},\Delta t)+i\mathbf{x}\cdot\mathbf{k}}\, d\mathbf{k}\,, \tag{1}$$

where $\phi(\mathbf{x},\mathbf{k},\Delta t)$ is the phase function. The mixed-domain operator is also referred to as the one-step wave extrapolation operator (Zhang and Zhang, 2009; Sun and Fomel, 2013). Be-

© 2014 SEG

DOI http://dx.doi.org/10.1190/segam2014-1588.1

Downloaded 11/06/14 to 128.210.3.233. Redistribution subject to SEG license or copyright; see Terms of Use at http://library.seg.org/

cause the wave extrapolation matrix is complex, it propagates a complex wavefield with the imaginary part being the Hilbert transform of the real part:

$$P(\mathbf{k},t) = P_r \pm F[H(p_r(\mathbf{x},t))] \,, \tag{2}$$

where P and P_r, respectively, denote the complex wavefield and real wavefield, and F denotes spatial Fourier transform.

Converting the dual-domain expression 1 into the space domain, we obtain

$$p(\mathbf{x},t+\Delta t) = \int p(\mathbf{y},t) \int e^{i\phi(\mathbf{x},\mathbf{k},\Delta t)+i\mathbf{k}\cdot(\mathbf{x}-\mathbf{y})}\, d\mathbf{k}\, d\mathbf{y} \,. \tag{3}$$

The adjoint form of operator 1 can be written as:

$$P(\mathbf{k},t) = \int p(\mathbf{x},t+\Delta t) e^{-i\phi(\mathbf{x},\mathbf{k},\Delta t)-i\mathbf{x}\cdot\mathbf{k}}\, d\mathbf{x} \,. \tag{4}$$

Expressing the dual domain operator 4 in the space domain and stepping forward in time, we arrive at a different operator:

$$p(\mathbf{x},t+\Delta t) = \int p(\mathbf{y},t) \int e^{i\phi(\mathbf{y},\mathbf{k},\Delta t)+i\mathbf{k}\cdot(\mathbf{x}-\mathbf{y})}\, d\mathbf{k}\, d\mathbf{y} \,. \tag{5}$$

The phase function in equation 3 depends on the output space $\mathbf{x}$, and thus represents a kind of non-stationary combination filter (Margrave, 1998). In comparison, the phase function appearing in equation 5 depends on the input space $\mathbf{y}$, and leads to a kind of non-stationary convolution filter. Both operators 3 and 5 apply the same wave-propagation phase function, $\phi(\mathbf{x},\mathbf{k},\Delta t)$; the one-step low-rank wave extrapolation operator 3 applies the phase function in the wavenumber domain after forward Fourier transform, whereas the new operator 5 applies the phase function in the space domain before the inverse Fourier transform. The essential difference between the two is that the non-stationary convolution has the physical interpretation of scaled, linear superposition of the non-stationary filter impulse responses, as suggested by Huygens' principle, whereas non-stationary combination filters do not have such implications (Margrave, 1998). The mixed-domain operator 3 is an equivalent to the most accurate limiting case of phase shift plus interpolation (PSPI) method (Gazdag and Squazzero, 1984; Kesinger, 1992), which has been a popular choice for one-way wavefield extrapolators. The proposed operator 5 is analogous to the non-stationary phase shift (NSPS) method of Margrave (1998) for one-way wave extrapolation.

The low-rank algorithm introduced by Fomel et al. (2013) is a separable approximation that selects a set of N representative spatial locations and M representative wavenumbers, which correspond to rows and columns from the original wave-propagation matrix. The low-rank one-step wave extrapolation uses low-rank decomposition to approximate the mixed-domain phase function in equation 3:

$$p(\mathbf{x},t+\Delta t) \approx \sum_{m=1}^{M} W(\mathbf{x},\mathbf{k}_m) \left(\sum_{n=1}^{N} a_{mn} \left(\int e^{i\mathbf{x}\cdot\mathbf{k}} W(\mathbf{x}_n,\mathbf{k}) P(\mathbf{k},t) d\mathbf{k} \right) \right) , \tag{6}$$

whose computational cost effectively equals that of applying N inverse fast Fourier transforms per time step, where N is the approximation rank and is typically a number less than ten.

With the help of low-rank decomposition, the computational effort for the new NSPS method can be made identical to that of the low-rank PSPI wave extrapolation, by approximating the wave propagation operator appearing in equation 5 with

$$P(\mathbf{k},t+\Delta t) \approx \sum_{n=1}^{N} W(\mathbf{x}_n,\mathbf{k}) \left(\sum_{m=1}^{M} a_{mn} \left(\int e^{-i\mathbf{x}\cdot\mathbf{k}} W(\mathbf{x},\mathbf{k}_m) p(\mathbf{x},t) d\mathbf{x} \right) \right) . \tag{7}$$

Note that, for simplicity, equations 6 and 7 left out an operation of the forward and inverse Fourier transforms.

The low-rank NSPS itself is a stable and accurate wave extrapolation operator and can be immediately useful for seismic modeling or migration. Following Ferguson and Margrave (2002), we further propose to use it jointly with low-rank PSPI wave extrapolation to devise a symmetric wave extrapolation operator that is more accurate in complex media. The motivation for the symmetric operator is that, as has been demonstrated above, operator 3 computes the wavefield at the next time step using only velocity from the output space, whereas operator 5 uses only velocity from the input space. A superior operator could be one that incorporates both pieces of information when making a time step. Let us denote the original low-rank PSPI operator (equation 6) as $\mathbf{P}$ and the proposed low-rank NSPS operator (equation 7) as $\mathbf{N}$. A symmetric way to formulate the wave extrapolation problem introduces the wavefield at the half time step:

$$\mathbf{N}^-_{\frac{\Delta t}{2}}\, p(\mathbf{x},t+\Delta t) = \mathbf{N}^+_{\frac{\Delta t}{2}}\, p(\mathbf{x},t) \tag{8}$$

Applying the pseudo-inverse of $N^-_{\frac{\Delta t}{2}}$, the following time-stepping scheme can be derived:

$$\begin{aligned} p(\mathbf{x},t+\Delta t) &= (\mathbf{N}^-_{\frac{\Delta t}{2}})^\dagger \mathbf{N}^+_{\frac{\Delta t}{2}}\, p(\mathbf{x},t) \\ &= [(\mathbf{N}^-_{\frac{\Delta t}{2}})^* \mathbf{N}^-_{\frac{\Delta t}{2}}]^{-1} (\mathbf{N}^-_{\frac{\Delta t}{2}})^* (\mathbf{N}^+_{\frac{\Delta t}{2}})\, p(\mathbf{x},t) \\ &\approx (\mathbf{N}^-_{\frac{\Delta t}{2}})^* (\mathbf{N}^+_{\frac{\Delta t}{2}})\, p(\mathbf{x},t) \\ &= \mathbf{P}^+_{\frac{\Delta t}{2}}\, \mathbf{N}^+_{\frac{\Delta t}{2}}\, p(\mathbf{x},t) \end{aligned} \tag{9}$$

The approximation is based on the assumption that the normal operator $(\mathbf{N}^-_{\frac{\Delta t}{2}})^* \mathbf{N}^-_{\frac{\Delta t}{2}}$ is close to the identity matrix when the time-step size or the velocity variation is small.

Based on the same approach, we can alternatively apply the low-rank PSPI operator for the first half step and NSPS for the second half step:

$$p(\mathbf{x},t+\Delta t) \approx \mathbf{N}^+_{\frac{\Delta t}{2}}\, \mathbf{P}^+_{\frac{\Delta t}{2}}\, p(\mathbf{x},t) \tag{10}$$

As will be demonstrated by the numerical examples, the resulting wavefield from operators 9 and 10 will acquire more accurate phase information. It is easy to verify that the adjoint of the proposed symmetric operator is itself with reversed sign of the phase function.

The low-rank NSPS can be employed as the adjoint of the one-step PSPI two-way wave extrapolation operator in LSRTM in order to improve the quality of seismic images (Zhang et al.,

© 2014 SEG

DOI http://dx.doi.org/10.1190/segam2014-1588.1

2013; Liu et al., 2013). Since our wave extrapolation kernel operates in the complex domain, we must have a proper definition of data and reflectivity with complex values. The analytical data follows the definition of the complex wavefield in equation 2, implying that the data need to be Hilbert transformed along the time axis and supplied as the imaginary part before the migration process. We then adopt the formulation of complex-valued cross-correlation imaging condition (Claerbout, 1985):

$$I(\mathbf{x}) = \sum_{s} \sum_{t} \bar{S}_s(\mathbf{x},t)\, R_s(\mathbf{x},t) \, , \tag{11}$$

where the lower case s denotes all the shots and t denotes all the time slices. Correspondingly, the imaging condition with source illumination compensation can be given as

$$I(\mathbf{x}) = \sum_{s} \frac{\sum_{t} \bar{S}_s(\mathbf{x},t)\, R_s(\mathbf{x},t)}{\sum_{t} \bar{S}_s(\mathbf{x},t)\, S_s(\mathbf{x},t)} \, . \tag{12}$$

NUMERICAL EXAMPLES

Symmetric wavefield extrapolation in a two-layer medium

So far we have introduced four kinds of wave extrapolation operators: the low-rank PSPI operator, the low-rank NSPS operator, and two hybrid operators using half of the time-step size. Which operator is capable of producing the most accurate wavefield extrapolation result? To make a fair comparison, we use the same time-step size for all four operators, and denote them using $\mathbf{P}_{1/2}\mathbf{P}_{1/2}$ for one-step PSPI, $\mathbf{N}_{1/2}\mathbf{N}_{1/2}$ for one-step NSPS, $\mathbf{N}_{1/2}\mathbf{P}_{1/2}$ for first NSPS then PSPI, and $\mathbf{P}_{1/2}\mathbf{N}_{1/2}$ for first PSPI then NSPS. We use a 2D, two-layer isotropic velocity model (Du et al., 2014), as demonstrated by Figure 1(a). The top layer has a velocity of 1500 m/s and the lower layer 4500 m/s, between which lies a sharp velocity discontinuity. The spatial sampling is 15 m along both vertical and horizontal directions. An explosive source (a Ricker wavelet) is located in the center of the model where $v = 1500\ m/s$. Assuming the source is excited at time $t = 0\ s$, wavefield snapshots using different propagators are taken at $t = 0.88\ s$.

Figure 1(b) shows a wavefield snapshot computed by the low-rank PSPI operator using a sufficiently small step size $\Delta t = 0.5\ ms$, which can be treated as a reference solution. The reference wavefield is overlaid by the first-arrival travel-time contour computed by solving the eikonal equation. The travel-time contour follows exactly the boundary between positive and negative amplitude, so that any misalignment of the boundary line and the travel-time contour can be an indication of timing error (inaccuracy of phase). Figures 1(c) to 1(f) are all computed using a time-step size of 16 ms, thus at an effective computational cost of 8 ms time step. Figure 1(c) is calculated by $\mathbf{P}_{1/2}\mathbf{P}_{1/2}$, showing positive timing error in the transmitted arrival. Figure 1(d) is calculated by $\mathbf{N}_{1/2}\mathbf{N}_{1/2}$, showing negative timing error in the transmitted arrival. Figures 1(e) and 1(f) are propagated by $\mathbf{N}_{1/2}\mathbf{P}_{1/2}$ and $\mathbf{P}_{1/2}\mathbf{N}_{1/2}$, respectively, and both transmitted arrivals display little timing error. The transmitted arrivals calculated by $\mathbf{P}_{1/2}\mathbf{P}_{1/2}$ and $\mathbf{N}_{1/2}\mathbf{N}_{1/2}$ acquire different amplitudes, whereas those calculated by $\mathbf{N}_{1/2}\mathbf{P}_{1/2}$ and $\mathbf{P}_{1/2}\mathbf{N}_{1/2}$ have identical amplitudes.

The computational costs of applying the four kinds of operators are almost the same; the $\mathbf{P}_{1/2}\mathbf{N}_{1/2}$ option comes with a slightly higher cost comparing with the other three, requiring one additional pair of FFTs, because PSPI first operates in the wavenumber domain and NSPS then operates in the space domain. Therefore, $\mathbf{N}_{1/2}\mathbf{P}_{1/2}$ becomes the most preferred choice among the four.

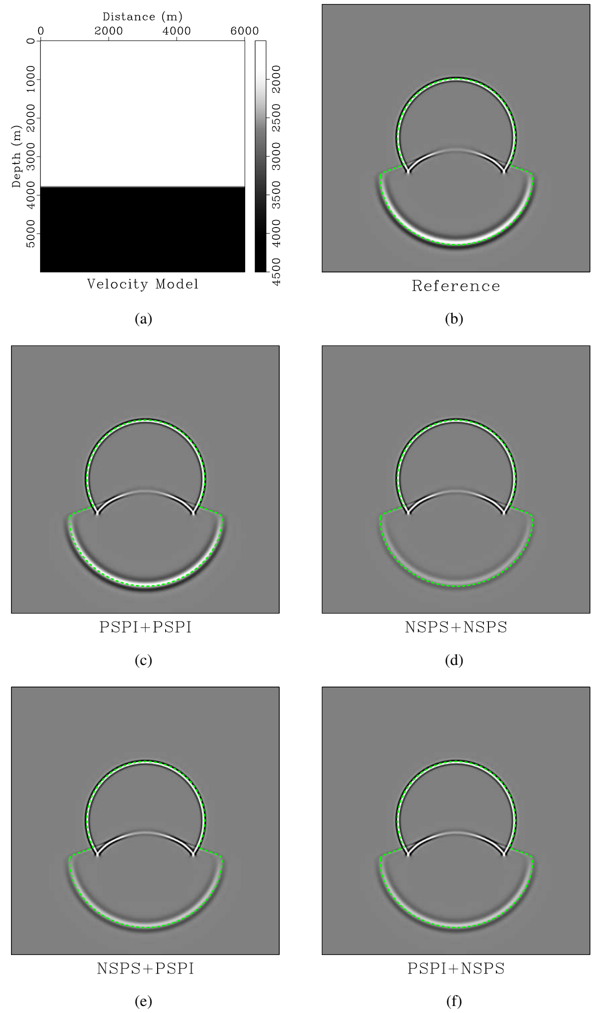

Figure 1: Accuracy comparison between different schemes. (a) Two-layer isotropic model; (b) reference wavefield snapshot overlaid by computed travel-time contour at 0.88 s; (c) to (f) wavefield snapshots computed by $\mathbf{P}_{1/2}\mathbf{P}_{1/2}$, $\mathbf{N}_{1/2}\mathbf{N}_{1/2}$, $\mathbf{N}_{1/2}\mathbf{P}_{1/2}$ and $\mathbf{P}_{1/2}\mathbf{N}_{1/2}$, respectively.

Least-squares Migration: the Sigsbee2A model

Our second example tests LSRTM using the Sigsbee2A model, shown in Figure 2. Fifty shots, starting at 3.28 km and ending at 26.80 km with an equal spacing of 0.48 km, are used to generate the images. The inversion process aims to minimize the least-squares norm of the data misfit. Cross-correlation imag-

Downloaded 11/06/14 to 128.210.3.233. Redistribution subject to SEG license or copyright; see Terms of Use at http://library.seg.org/

© 2014 SEG

DOI http://dx.doi.org/10.1190/segam2014-1588.1

Downloaded 11/06/14 to 128.210.3.233. Redistribution subject to SEG license or copyright; see Terms of Use at http://library.seg.org/

ing condition is used. Figure 3 compares the results generated by low-rank RTM and low-rank LSRTM. The image produced by RTM suffers from some artifacts, especially at locations near the top of the salt, as a result of the limited source coverage. After several conjugate gradient iterations with a zero starting model, the image produced by LSRTM successfully suppresses the artifacts present in the RTM image, does a better delineating reflectors such as the salt body, and enhances the illumination of deeper reflectors. Other artifacts such as back-scattered noise are suppressed as well. Figure 4 zooms in on the salt body, demonstrating the area where LSRTM effectively suppresses the artifacts from a single RTM process. The proposed LSRTM framework can further incorporate a regularization scheme to enforce model constraints (Xue et al., 2014).

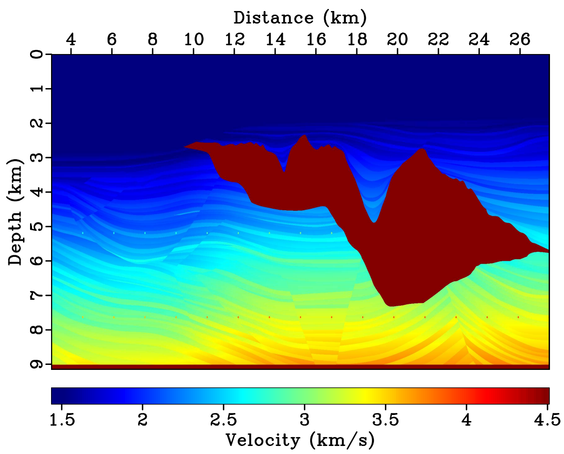

Figure 2: The Sigsbee2A velocity model.

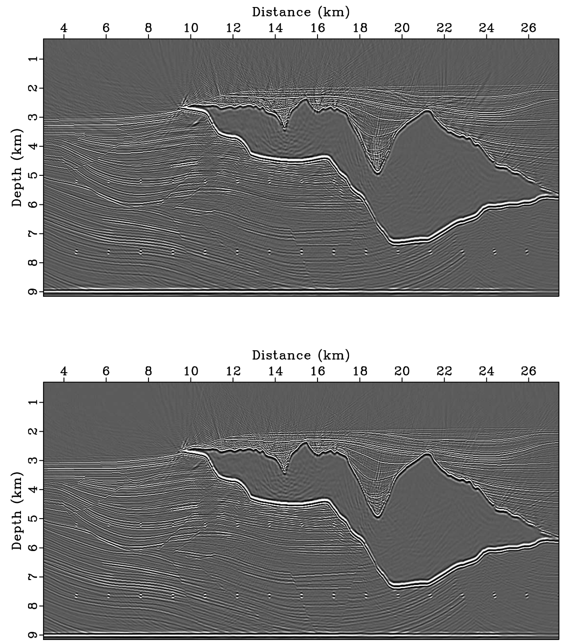

Figure 3: A comparison between the image produced by regular low-rank RTM (top) and low-rank LSRTM (bottom).

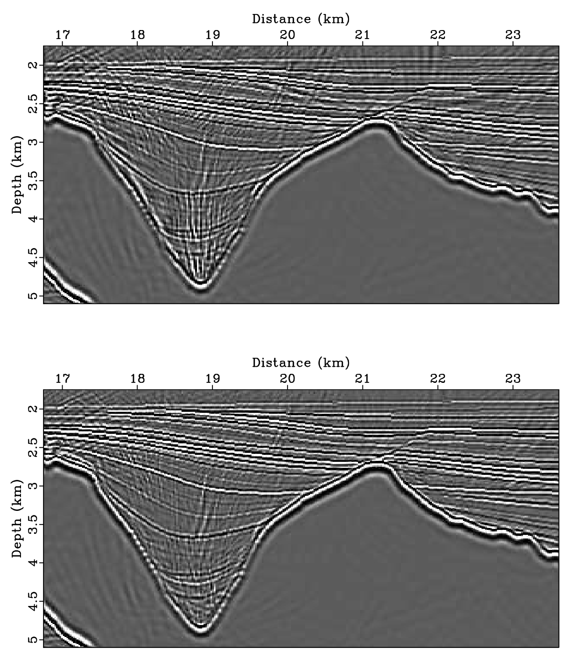

Figure 4: Zoomed-in sections of the RTM image (top) and LSRTM image (bottom). Compared with the RTM image, the image produced by LSRTM is not only cleaner, but also more uniformly illuminated.

CONCLUSIONS

Based on the theory of non-stationary filtering, we propose the low-rank NSPS operator, which is related to the adjoint of the low-rank PSPI operator. The NSPS operator is a non-stationary convolution filter and can be interpreted as a superposition of non-stationary impulse responses. We further propose to combine PSPI and NSPS operators to construct a symmetric one-step two-way wave extrapolation operator that is capable of propagating wavefields with an improved accuracy. Low-rank one-step wave extrapolation and its adjoint can be incorporated into LSRTM, improving the quality of the final image.

ACKNOWLEDGMENTS

We thank Lexing Ying for inspiring discussions. We thank Statoil and other sponsors of the Texas Consortium for Computation Seismology (TCCS) for financial support. We thank TACC (Texas Advanced Computing Center) for providing computational resources.

DOI http://dx.doi.org/10.1190/segam2014-1588.1

http://dx.doi.org/10.1190/segam2014-1588.1

EDITED REFERENCES

Note: This reference list is a copy-edited version of the reference list submitted by the author. Reference lists for the 2014 SEG Technical Program Expanded Abstracts have been copy edited so that references provided with the online metadata for each paper will achieve a high degree of linking to cited sources that appear on the Web.

REFERENCES

Baysal, E., D. D. Kosloff, and J. W. C. Sherwood, 1983, Reverse-time migration: Geophysics, **48**, 1514–1524, http://dx.doi.org/10.1190/1.1441434.

Chu, C., and P. L. Stoffa, 2010, Acoustic anisotropic wave modeling using normalized pseudoLaplacian: 80th Annual International Meeting, SEG, Expanded Abstracts, 2972–2976.

Claerbout, J. F., 1985, Imaging the earth's interior: Blackwell Scientific Publications.

Dai, W., X. Wang, and G. T. Schuster, 2011, Least-squares migration of multisource data with a deblurring filter: Geophysics, **76**, no. 5, R135–R146, http://dx.doi.org/10.1190/geo2010-0159.1.

Du, X., R. P. Fletcher, and P. J. Fowler, 2010, Pure P-wave propagators versus pseudo-acoustic propagators for RTM in VTI media: Presented at the 72nd Annual International Conference and Exhibition, EAGE.

Du, X., P. J. Fowler, and R. P. Fletcher, 2013, Recursive integral time-extrapolation methods for waves: A comparative review: Geophysics, **79**, no. 1, T9–T26, http://dx.doi.org/10.1190/geo2013-0115.1.

Etgen, J., and S. Brandsberg-Dahl, 2009, The pseudo-analytical method: application of pseudoLaplacians to acoustic and acoustic anisotropic wave propagation: 79th Annual International Meeting, SEG, Expanded Abstracts, 2552–2556.

Farmer, P. A., I. F. Jones, H. Zhou, R. I. Bloor, and M. C. Goodwin, 2006, Application of reverse-time migration to complex imaging problems: First Break, **24**, 65–73.

Ferguson, R. J., and G. F. Margrave, 2002, Prestack depth migration by symmetric nonstationary phase shift: Geophysics, **67**, 594–603, http://dx.doi.org/10.1190/1.1468620.

Fletcher, R. P., X. Du, and P. J. Fowler, 2009, Reverse-time migration in tilted transversely isotropic (TTI) media: Geophysics, **74**, no. 6, WCA179–WCA187, http://dx.doi.org/10.1190/1.3269902.

Fomel, S., L. Ying, and X. Song, 2013, Seismic wave extrapolation using low-rank symbol approximation: Geophysical Prospecting, **61**, no. 3, 526–536, http://dx.doi.org/10.1111/j.1365-2478.2012.01064.x.

Fowler, P. J., X. Du, and R. P. Fletcher, 2010a, Coupled equations for reverse-time migration in transversely isotropic media: Geophysics, **75**, no. 1, S11–S22, http://dx.doi.org/10.1190/1.3294572.

Fowler, P. J., X. Du, and R. P. Fletcher, 2010b, Recursive integral time extrapolation methods for scalar waves: 80th Annual International Meeting, SEG, Expanded Abstracts, 3210–3215.

Gazdag, J., and P. Squazzero, 1984, Migration of seismic data by phase shift plus interpolation: Geophysics, **49**, 124–131, http://dx.doi.org/10.1190/1.1441643.

Kesinger, W., 1992, Extended split-step Fourier migration: 62nd Annual International Meeting, SEG, Expanded Abstracts, 917–920.

Kosloff, D., and E. Baysal, 1982, Forward modeling by a Fourier method: Geophysics, **47**, 1402–1412, http://dx.doi.org/10.1190/1.1441288.

Downloaded 11/06/14 to 128.210.3.233. Redistribution subject to SEG license or copyright; see Terms of Use at http://library.seg.org/

Downloaded 11/06/14 to 128.210.3.233. Redistribution subject to SEG license or copyright; see Terms of Use at http://library.seg.org/

Liu, F., S. A. Morton, S. Jiang, L. Ni, and J. P. Leveille, 2009, Decoupled wave equations for P- and SV-waves in an acoustic VTI media: 79th Annual International Meeting, SEG, Expanded Abstracts, 2844–2848.

Liu, Y., W. W. Symes, and Z. Li, 2013, Multisource least-squares extended reverse-time migration with preconditioning guided gradient method: 83rd Annual International Meeting, SEG, Expanded Abstracts, doi: 10.1190/segam2013-1251.1.

Margrave, G. F., 1998, Theory of nonstationary linear filtering in the Fourier domain with application to time-variant filtering: Geophysics, **63**, 244–259, http://dx.doi.org/10.1190/1.1444318.

Margrave, G. F., and R. J. Ferguson, 1999, Wavefield extrapolation by nonstationary phase shift: Geophysics, **64**, 1067–1078, http://dx.doi.org/10.1190/1.1444614.

McMechan, G. A., 1983, Migration by extrapolation of time-dependent boundary values: Geophysical Prospecting, **31**, no. 3, 413–420, http://dx.doi.org/10.1111/j.1365-2478.1983.tb01060.x.

Nemeth, T., C. Wu, and G. Schuster, 1999, Least-squares migration of incomplete reflection data: Geophysics, **64**, 208–221, http://dx.doi.org/10.1190/1.1444517.

Paffenholz, J., B. McLain, J. Zaske, and P. J. Keliher, 2002, Subsalt multiple attenuation and imaging: Observations from the Sigsbee2B synthetic data set: Presented at the 82nd Annual International Meeting, SEG.

Pestana, R. C., and P. L. Stoffa, 2010, Time evolution of the wave equation using rapid expansion method: Geophysics, **75**, no. 4, T121–T131, http://dx.doi.org/10.1190/1.3449091.

Reshef, M., D. Kosloff, M. Edwards, and C. Hsiung, 1988, Three-dimensional acoustic modeling by the Fourier method: Geophysics, **53**, 1175–1183, http://dx.doi.org/10.1190/1.1442557.

Ronen, S., and C. L. Liner, 2000, Least-squares DMO and migration: Geophysics, **65**, 1364–1371, http://dx.doi.org/10.1190/1.1444827.

Song, X., S. Fomel, and L. Ying, 2013, Low-rank finite-differences and low-rank Fourier finite-differences for seismic wave extrapolation: Geophysical Journal International, **193**, no. 2, 960–969, http://dx.doi.org/10.1093/gji/ggt017.

Soubaras, R., and Y. Zhang, 2008, Two-step explicit marching method for reverse time migration: 78th Annual International Meeting, SEG, Expanded Abstracts, 2272–2276.

Stoffa, P. L., and R. C. Pestana, 2009, Numerical solution of the acoustic wave equation by the rapid expansion method (REM) — A one-step time evolution algorithm: 79th Annual International Meeting, SEG, Expanded Abstracts, 2672–2676.

Sun, J., and S. Fomel, 2013, Low-rank one-step wave extrapolation: 83rd Annual International Meeting, SEG, Expanded Abstracts, doi: 10.1190/segam2013-1123.1.

Tang, Y., 2009, Target-oriented wave-equation least-squares migration/inversion with phase-encoded Hessian: Geophysics, **74**, no. 6, WCA95–WCA107, http://dx.doi.org/10.1190/1.3204768.

Ward, B. D., G. F. Margrave, and M. P. Lamoureux, 2008, Phase-shift time-stepping for reverse-time migration: 78th Annual International Meeting, SEG, Expanded Abstracts, 2262–2266.

Whitmore, N. D., 1983, Iterative depth migration by backward time propagation: 53rd Annual International Meeting, SEG, Expanded Abstracts, 382–385.

© 2014 SEG

DOI http://dx.doi.org/10.1190/segam2014-1588.1

Xue, Z., Y. Chen, S. Fomel, and J. Sun, 2014, Imaging incomplete data and simultaneous-source data using least-squares reverse-time migration with shaping regularization: Presented at the 84th Annual International Meeting, SEG.

Zhang, Y., L. Duan, and Y. Xie, 2013, A stable and practical implementation of least-squares reverse-time migration: 83rd Annual International Meeting, SEG, Expanded Abstracts, doi: 10.1190/segam2013-0577.1.

Zhang, Y., and G. Zhang, 2009, One-step extrapolation method for reverse time migration: Geophysics, **74**, no. 4, A29–A33, http://dx.doi.org/10.1190/1.3123476.

Zhang, Y., G. Zhang, D. Yingst, and J. Sun, 2007, Explicit marching method for reverse-time migration: 77th Annual International Meeting, SEG, Expanded Abstracts, 2300–2303.

Downloaded 11/06/14 to 128.210.3.233. Redistribution subject to SEG license or copyright; see Terms of Use at http://library.seg.org/

© 2014 SEG

DOI http://dx.doi.org/10.1190/segam2014-1588.1